Theoretical Studies on Ru-Catalyzed Pauson−Khand-Type [2+2+1] and Related [2+2+1+1] Cycloadditions

Can Wang[†] and Yun-Dong Wu*[,†,‡]

National Laboratory of Molecular Science, College of Chemistry, Peking University, Beijing 100871, People's Republic of China, and Department of Chemistry, The Hong Kong University of Science and Technology, Clear Water Bay, Kowloon, Hong Kong, People's Republic of China

Received May 9, 2008

Density functional theory (DFT) calculations have been carried out to understand the mechanism of the $Ru_3(CO)_{12}$-catalyzed Pauson−Khand-type [2+2+1] reaction and related [2+2+1+1] cycloadditions. The geometries were optimized using the BP86/6-31G*(SDD for Ru) method, and the energies were evaluated with the 6-311+G*(SDD) basis set. We found that these reactions are initiated by a CO−alkyne coupling, forming a ruthenacyclobutenone intermediate, and the widely accepted alkene−alkyne coupling pathway has a much higher activation energy. In the intermolecular reaction between alkene and alkyne, the formation of quinones and hydroquinones through [2+2+1+1] cycloadditions is more favorable than the Pauson−Khand-type reaction, while the intramolecular reaction with 1,6-enyne leads to a favorable Pauson−Khand-type reaction. These results are in agreement with experimental observations. For the [2+2+1+1] cycloadditions we found that the formation of quinones is favored over the formation of hydroquinones due to the preferred insertion of alkynes, which can be attributed to the preferred orbital interaction between the π orbital of the alkyne moiety and the d orbital of the metal center.

Introduction

Cycloadditions of small chemical building blocks[1] are very important in organic synthesis due to the possibility of constructing straightforward ring compounds and the fact that they are atom-economic.[2] The Pauson−Khand reaction,[3] which combines alkene, alkyne, and carbon monoxide molecules into a cyclopentenone ring, has been widely studied and extensively applied in organic synthesis.[4] Originally, the reaction was mediated by $Co_2(CO)_8$ with a stoichiometric consumption of the metal complex.[5] In the past two decades, this type of reaction was found to be accelerated by a few ligands[6] and catalyzed by many transition metal complexes.[7] Among them, $Ru_3(CO)_{12}$ is an interesting example. In 1997, Mitsudo's[8a] and Murai's[8b] groups simultaneously found that $Ru_3(CO)_{12}$ could catalyze the intramolecular Pauson−Khand reaction under high temperature and high carbon monoxide pressure (Scheme 1). In their attempt to use this catalyst for intermolecular Pauson−Khand reactions, Mitsudo's group did not get the expected cyclopentenone product. Instead, [2+2+1+1] cycloaddition products, hydroquinones and quinines, were obtained in considerable yields (Scheme 2).[9a] The findings were important because those two aromatic compounds are of great use in industry.[10] For example,

* Corresponding author. E-mail: chydwu@ust.hk.
† Peking University.
‡ The Hong Kong University of Science and Technology.

(1) Reviews of metal-catalyzed cycloadditions: (a) D'Souza, D. M.; Muller, T. J. J. *Chem. Soc. Rev.* **2007**, *36*, 1095–1108. (b) Chopade, P. R.; Louie, J. *Adv. Synth. Catal.* **2006**, *348*, 2307–2327. (c) Kotha, S.; Brahmachary, E.; Lahiri, K. *Eur. J. Org. Chem.* **2005**, 4741. (d) Montgomery, J. *Acc. Chem. Res.* **2000**, *33*, 467. (e) Fruhauf, H.-W. *Chem. Rev.* **1997**, *97*, 523. (f) Ojima, I.; Tzamarioudaki, M.; Li, Z.; Donovan, R. J. *Chem. Rev.* **1996**, *96*, 635. (g) Lautens, M.; Klute, W.; Tam, W. *Chem. Rev.* **1996**, *96*, 49.

(2) (a) Trost, B. M. *Acc. Chem. Res.* **2002**, *35*, 695. (b) Trost, B. M. *Angew. Chem., Int. Ed. Engl.* **1995**, *34*, 259–281.

(3) (a) Gibson, S. E.; Mainolfi, N. *Angew. Chem., Int. Ed.* **2005**, *44*, 3022. (b) Bonaga, L. V. R.; Krafft, M. E. *Tetrahedron* **2004**, *60*, 9795. (c) Blanco-Urgoiti, J.; Anorbe, L.; Perez-Serrano, L.; Dominguez, G.; Perez-Castells, J. *Chem. Soc. Rev.* **2004**, *33*, 32. (d) Alcaide, B.; Almendros, *Eur. J. Org. Chem.* **2004**, 3377. (e) Gibson, S. E.; Stevenazzi, A. *Angew. Chem., Int. Ed.* **2003**, *42*, 1800. (f) Rivero, M. R.; Adrio, J.; Carretero, J. C. *Eur. J. Org. Chem.* **2002**, 2881. (g) Fletcher, A. J.; Christie, S. D. R. *J. Chem. Soc., Perkin Trans. 1* **2000**, 1657. (h) Brummond, K. M.; Kent, J. L. *Tetrahedron* **2000**, *56*, 3263. (i) Chung, Y. K. *Coord. Chem. Rev.* **1999**, *188*, 297. (j) Geis, O.; Schmalz, H. G. *Angew. Chem., Int. Ed.* **1998**, *37*, 911.

(4) (a) Kozaka, T.; Miyakoshi, N.; Mukai, C. *J. Org. Chem.* **2007**, *72*, 10147. (b) Min, S. J.; Danishefsky, S. J. *Angew. Chem., Int. Ed.* **2007**, *46*, 2199. (c) Crawford, J. J.; Kerr, W. J.; McLaughlin, M.; Morrison, A. J.; Pauson, P. L.; Thurston, G. J. *Tetrahedron* **2006**, *62*, 11360. (d) Ishizaki, M.; Niimi, Y.; Hoshino, O.; Hara, H.; Takahashi, T. *Tetrahedron* **2005**, *61*, 4053. (e) Caldwell, J. J.; Cameron, I. D.; Christie, S. D. R.; Hay, A. M.; Johnstone, C.; Kerr, W. J.; Murray, A. *Synthesis-Stuttgart* **2005**, 3293.

(5) (a) Khand, I. U.; Knox, G. R.; Pauson, P. L.; Watts, W. E.; Foreman, M. I. *J. Chem. Soc., Perkin Trans. 1* **1973**, 977–981. (b) Khand, I. U.; Knox, G. R.; Pauson, P. L.; Watts, W. E. *J. Chem. Soc., Chem. Commun.* **1971**, 36.

(6) (a) Tang, Y.; Deng, L.; Zhang, Y.; Dong, G.; Chen, J.; Yang, Z. *Org. Lett.* **2005**, *7*, 593–595. (b) Sugihara, T.; Yamaguchi, M.; Nishizawa, M. *Chem.−Eur. J.* **2001**, *7*, 1589–1595. (c) Sugihara, T.; Yamada, M.; Yamaguchi, M.; Nishizawa, M. *Synlett* **1999**, 771. (d) Sugihara, T.; Yamaguchi, M. *Synlett* **1998**, 1384. (e) Sugihara, T.; Yamada, M.; Ban, H.; Yamaguchi, M.; Kaneko, C. *Angew. Chem., Int. Ed.* **1998**, *36*, 2801. (f) Chung, Y. K.; Lee, B. Y.; Jeong, N.; Hudecek, M.; Pauson, P. L. *Organometallics* **1993**, *12*, 220. (g) Billington, D. C.; Helps, I. M.; Pauson, P. L.; Thomson, W.; Willison, D. *J. Organomet. Chem.* **1988**, *354*, 233.

(7) Titnium: (a) Hicks, F. A.; Kablaoui, N. M.; Buchwald, S. L. *J. Am. Chem. Soc.* **1999**, *121*, 5881. (b) Hicks, F. A.; Buchwald, S. L. *J. Am. Chem. Soc.* **1999**, *121*, 7026. Molybdenum: (c) Jeong, N.; Lee, S. J.; Lee, B. Y.; Chung, Y. K. *Tetrahedron Lett.* **1993**, *34*, 4027. (d) Adrio, J.; Rivero, M. R.; Carretero, J. C. *Org. Lett.* **2005**, *7*, 431. (e) Brummond, K. M.; Kerekes, A. D.; Wan, H. *J. Org. Chem.* **2002**, *67*, 5156Ruthenium: (f) Kondo, T.; Suzuki, N.; Okada, T.; Mitsudo, T. *J. Am. Chem. Soc.* **1997**, *119*, 6187. (g) Morimoto, T.; Fuji, K.; Tsutsumi, K.; Kakiuchi, K. *J. Am. Chem. Soc.* **2002**, *124*, 3806Iridium: (h) Shibata, T.; Takagi, K. *J. Am. Chem. Soc.* **2000**, *122*, 9852Rhodium: (i) Jeong, N. *Organometallics* **1998**, *17*, 3642. (j) Jeong, N.; Sung, B. K.; Choi, Y. K. *J. Am. Chem. Soc.* **2000**, *122*, 6771. (k) Mukai, C.; Inagaki, F.; Yoshida, T.; Yoshitani, K.; Hara, Y.; Kitagaki, S. *J. Org. Chem.* **2005**, *70*, 7159.

(8) (a) Kondo, T.; Suzuki, N.; Okada, T.; Mitsudo, T. *J. Am. Chem. Soc.* **1997**, *119*, 6187. (b) Morimoto, T.; Chatani, N.; Fukumoto, Y.; Murai, S. *J. Org. Chem.* **1997**, *62*, 3762.

10.1021/om8004178 CCC: $40.75
Publication on Web 11/07/2008

Scheme 1. Ru-Complex-Catalyzed Pauson−Khand-Type Reaction

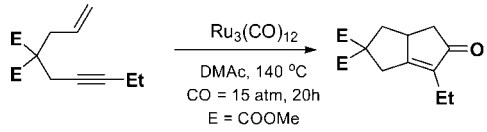

Scheme 2. Ru-Complex-Catalyzed [2+2+1+1] Cycloaddition Reactions

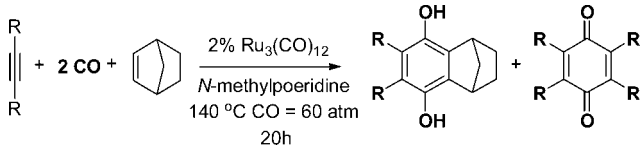

hydroquinones are very effective photographic developers and are used extensively as antioxidants. Quinones find uses as polymer inhibitors and as intermediates for numerous dyes. Recently, an optimized catalyst with a better substrate tolerance for [2+2+1+1] cycloaddition was reported.[9b] It is thus interesting to determine how these different products are generated to develop the reactions further.

It is generally accepted that Pauson−Khand-type reactions proceed through the coupling of alkene and alkyne on the metal center, followed by the insertion of a CO molecule and reductive elimination (Scheme 3, path A), as proposed for the original Pauson−Khand reaction catalyzed by $Co_2(CO)_8$.[11] However, with the alternation of the reacting order, in principle there are at least two other possibilities, namely, the coupling between CO and alkyne followed by alkene insertion, or coupling between CO and alkene followed by the alkyne insertion, both yielding cyclopentenone after reductive elimination (Scheme 3, paths B and C). Though these alternative mechanisms seem unlikely at first glance, they become more valid with the [2+2+1+1] cycloadditions. If there are no concerted pathways to generate the [2+2+1+1] products, the reactions are very likely to be initiated by the coupling between CO and alkene or alkyne. As shown in Scheme 3, the easiest ways to assemble a hydroquinone and a quinone molecule are via pathways D (the product will tautomerize to generate a hydroquinone molecule) and E. Indeed, metallacyclobutenone intermediates through the coupling between CO and alkyne were proposed with support from spectroscopic analyses,[12] though the highly strained four-membered metallacycles are scarce. In this paper we present a theoretical study of different reaction pathways and propose that all these reactions are initiated by the formation of the ruthenacyclobutenone intermediate.[13]

As early as 1983, Pomeroy and co-workers reported that ruthenium pentacarbonyls could be obtained by heating $Ru_3(CO)_{12}$ at elevated temperatures and elevated carbon monoxide pressure.[15] Since the Pauson−Khand-type [2+2+1] cycloaddition and the [2+2+1+1] cycloadditions were carried out under similar conditions to those in Pomeroy's experiments, we believe that $Ru_3(CO)_{12}$ (**1**) should be in equilibrium with $Ru(CO)_5$ (perhaps through $Ru(CO)_4$, **2**), which we use as a reference compound.

Computational Details

All calculations were carried out with the G03 program.[16] The geometries were fully optimized by the density functional theory (DFT) method of BP86.[17] We chose BP86 because this functional appears to perform well for transition metal complexes with carbonyl ligands.[18] The 6-31G* basis set was used for C, H, and O atoms, and Stuttgart/Dresden's pseudopotential SDD basis set[19] was used for the Ru atom. Intermediates and transition structures were confirmed by their vibrational frequency calculations. Single-point energies were also calculated with the 6-311+G* basis set for C, H, and O. All energies were zero-point energy corrected, and the free energies were evaluated using the same method used for geometric optimization. Thermal corrections were made on all compounds at their experimental temperatures. The solvent effects of DMac (*N,N*-dimethylacetamide, with a dielectric constant of 38) and toluene were also evaluated using the IEF-PCM method[20] as implemented in G03. The calculated absolute energies of all species are given in the Supporting Information. A few key structures have been further optimized by the larger basis set 6-311+G* (for details, see Supporting Information). We found that energies of all the testing structures are systematically decreased by less than 0.5 kcal/mol and free energies by less than 1.0 kcal/mol. Therefore we believe our choice of basis sets is accurate enough to investigate the system.

Results and Discussions

1. Model Studies of the Whole Free Energy Surface. Pauson−Khand-Type Reaction. By employing acetylene and ethylene as model compounds, we first studied the free energy profile for the three pathways. The intramolecular reaction for the 1,6-enyne substrate will be presented later.

Alkyne−Alkene Coupling Pathway. Since almost all previously proposed mechanisms for the Pauson−Khand-type reactions were through an alkyne−alkene coupling,[3,21] we studied this pathway first. Figure 1 shows the calculated free energy

(9) (a) Suzuki, N.; Kondo, T.; Mitsudo, T. *Organometallics* **1998**, *17*, 766. (b) Fukuyama, T.; Yamaura, R.; Higashibeppu, Y.; Okamura, T.; Ryu, I.; Kondo, T.; Mitsudo, T. *Org. Lett.* **2005**, *7*, 5781.

(10) Weissermel, K.; Arpe, H.-J. *Industrial Organic Chemistry*, 4th ed.; Wiley-VCH: Weinheim, Germany, 2003; p 363.

(11) Magnus, P.; Principe, L.-M. *Tetrahedron Lett.* **1985**, *26*, 4851. (b) Magnus, P.; Exon, C.; Robertson, A. *Tetrahedron* **1985**, *41*, 5861.

(12) (a) Mao, T.; Zhang, Z.; Washington, J.; Takats, J.; Jordan, R. B. *Organometallics* **1999**, *18*, 2331. (b) Macgregor, S. A.; Wenger, E. *J. Organomet. Chem.* **2000**, *607*, 164. (c) Mito, S.; Takahashi, T. *Chem. Commun.* **2005**, 2495. (d) Periasamy, M.; Pameshkumar; Radhakrishnan, U.; Brunet, J.-J. *J. Org. Chem.* **1998**, *63*, 4930.

(13) In an intermolecular Pauson−Khand-type reaction between alkynes and pyridylsilyl-substituted alkenes catalyzed by $Ru_3(CO)_{12}$, Itami and coworkers observed an intermediate of alkyne−alkene coupling.[14] We believe that the preference of this pathway originates from the special metal-coordinating ability of the pyridylsilyl-substituted alkenes. This will be studied and reported separately.

(14) Itami, K.; Mitsudo, K.; Fujita, K.; Ohashi, Y.; Yoshida, J. *J. Am. Chem. Soc.* **2004**, *126*, 11058–11066.

(15) Rushman, P.; van Buuren, G. N.; Shiralian, M.; Pomeroy, R. K. *Organometallics* **1983**, *2*, 693.

(16) Frisch, M. J. *Gaussian 03, revision C.02*; Gaussian, Inc.: Wallingford, CT, 2004.

(17) (a) Becke, A. D. *Phys. Rev. A* **1988**, *38*, 3098. (b) Perdew, J. P. *Phys. Rev. B* **1986**, *33*, 8822–8824.

(18) (a) Jonas, V.; Thiel, W. *J. Chem. Phys.* **1995**, *102*, 8474. (b) Li, J.; Schreckenbach, G.; Ziegler, T. *J. Am. Chem. Soc.* **1995**, *117*, 486. (c) van Wüllen, C. *J. Chem. Phys.* **1996**, *105*, 5485. (d) Szilagyi, R. K.; Frenking, G. *Organometallcs* **1997**, *22*, 4807. (e) Gonzáles-Blanco, O.; Branchadell, C. *J. Chem. Phys.* **1999**, *110*, 778. (f) Kenny, J. P.; King, R. B.; Schaefer, H. F. *Inorg. Chem.* **2001**, *40*, 900.

(19) (a) Andrae, D.; Haussermann, U.; Dolg, M.; Stoll, H.; Preuss, H. *Theor. Chim. Acta* **1990**, *77*, 123. (b) Dolg, M.; Wedig, U.; Stoll, H.; Preuss, H. *J. Chem. Phys.* **1987**, *86*, 866.

(20) (a) Mennucci, B.; Tomasi, J. *J. Chem. Phys.* **1997**, *106*, 5151. (b) Mennucci, B.; Cances, E.; Tomasi, J. *J. Phys. Chem. B* **1997**, *101*, 10506. (c) Tomasi, J.; Mennucci, B.; Cances, E. *J. Mol. Struct. (THEOCHEM)* **1999**, *464*, 211. (d) Chipman, D. M. *J. Chem. Phys.* **2000**, *112*, 5558. (e) Cances, E.; Mennucci, B. *J. Chem. Phys.* **2001**, *114*, 4744.

Scheme 3. Possible Pathways Involved in the Reaction of Acetylene, Ethylene, and CO Catalyzed by the Ru Complex

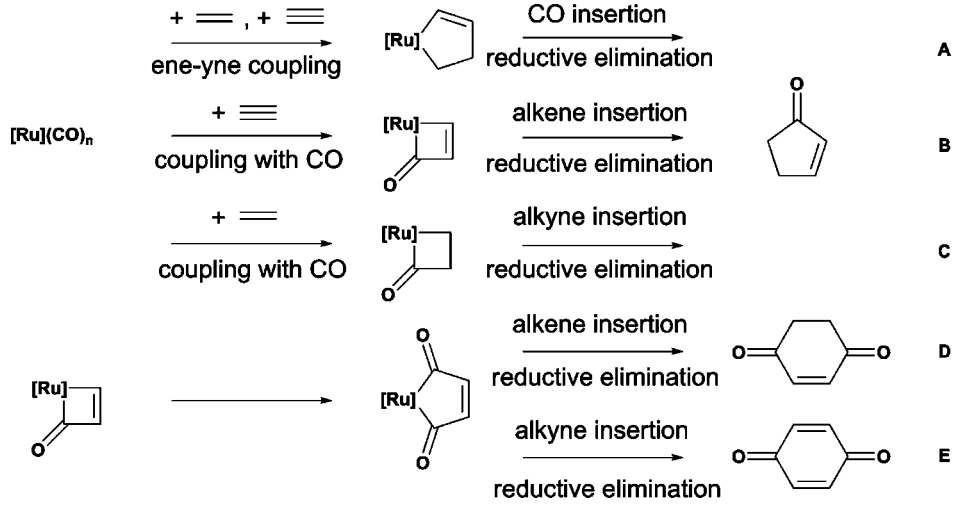

profile of the oxidative coupling pathway. The exchange of a CO ligand with an acetylene molecule requires about 10.0 kcal/mol. The subsequent exchange of another CO ligand with an ethylene molecule requires a further 14.9 kcal/mol, which amounts to about 24.9 kcal/mol relative to the reference compound **3**. The activation free energy for the subsequent oxidative coupling between acetylene and ethylene is about 17.0 kcal/mol, 41.9 kcal/mol overall. The resulting intermediate **7** is exogonic by about 17.5 kcal/mol with respect to **5**, but endogonic by about 7.4 kcal/mol with respect to **3**. The barrier of 41.9 kcal/mol is too high for the reaction to take place under the reaction temperature. Intermediate **7** can then bind another molecule of CO to form **10**, with a stabilization of about 12.7 kcal/mol in terms of free energy. The subsequent insertion of CO needs to overcome a barrier as high as 28.3 kcal/mol. After capturing another molecule of CO, **11** undergoes a reductive elimination to yield product **13**. The reaction free energy is about −24.9 kcal/mol with respect to **3**. Although direct reductive elimination of **10** through transition state **12ts-a** has a barrier as low as about 6.9 kcal/mol in terms of free energy, it is not as favorable as the pathway through **12ts** since the binding of CO stabilizes the system significantly.

Figure 2 shows the structures of various intermediates and transition states in the pathway. The reactant $Ru(CO)_5$ has a trigonal-bipyramidal geometry, which belongs to the D_{3h} point group. The calculated bond lengths are in good agreement with experimental values.[22] The 16-valence-electron (VE) $Ru(CO)_4$ is not square planar, as had been pointed out in previous calculations.[23] It had also been pointed out that $Ru(CO)_4$ should adopt a singlet configuration. The calculated structure displays a C_{2v} symmetry. When acetylene coordinates to **2**, the apical CO ligands tilt toward the acetylene and the equatorial CO ligands fold away. The exchange of a molecule of CO with a molecule of ethylene will afford two important structures. One is quasi-square-pyramidal and the other quasi-trigonal-bipyramidal. The latter one, **5-a**, is about 1.3 kcal/mol more stable

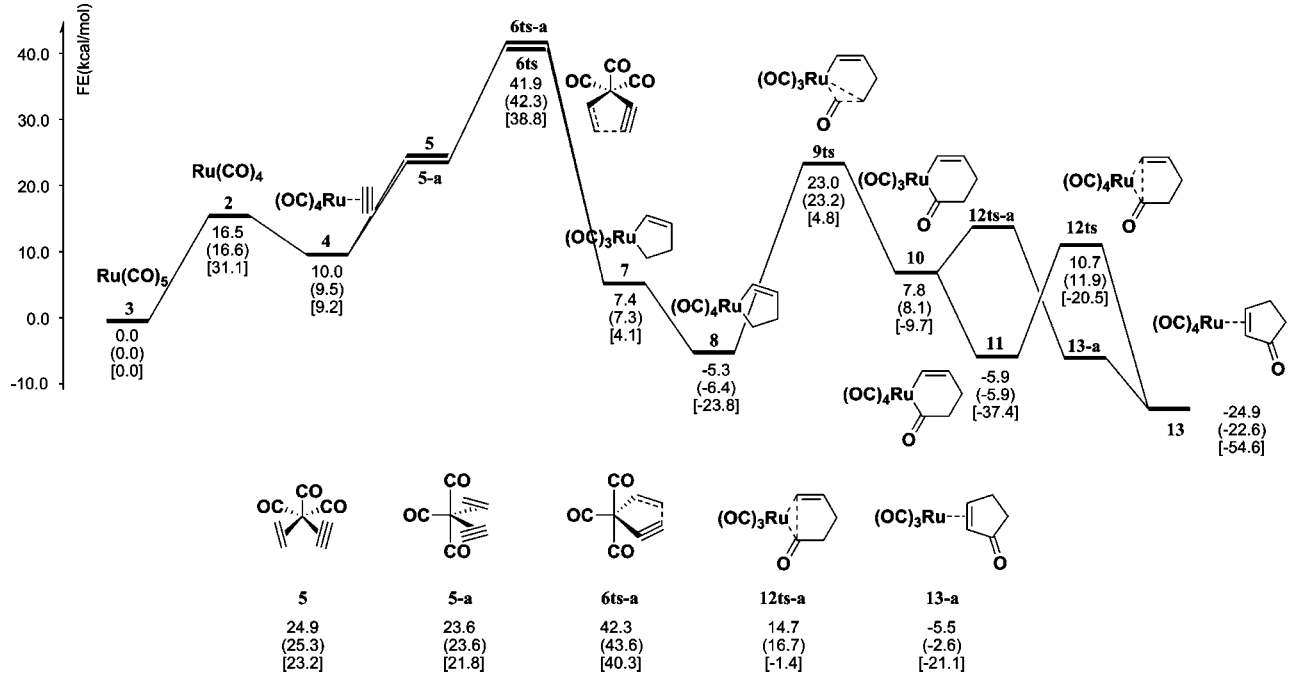

Figure 1. Free energy profile of the alkyne−alkene coupling pathway. Polarization solvent effects were added for all compounds. Free energies without solvent effects are in parentheses, and energies with ZPE are in square brackets. (The same order applies in other profiles.)

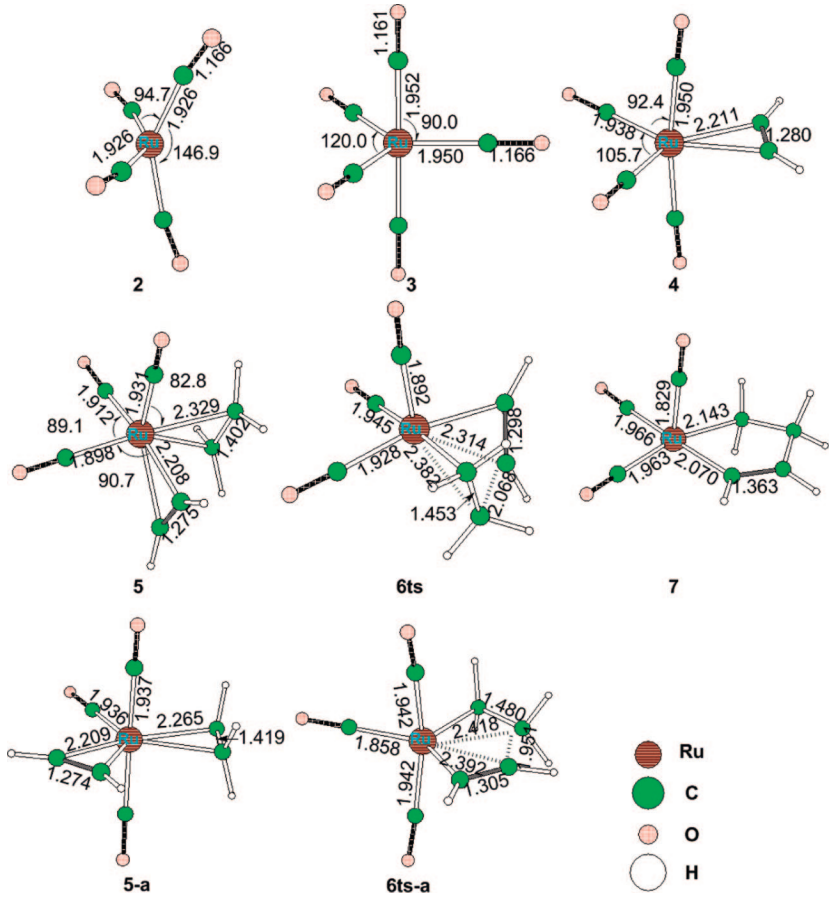

Figure 2. Structures for the alkene−alkyne coupling pathway.

than **5**. However, the quasi-square-pyramidal transition state **6ts** is slightly more favored over its quasi-trigonal-bipyramidal counterpart **6ts-a**, indicating that the square-pyramidal structure is more suitable for oxidative coupling reactions. The two resulting intermediates converge to a quasi-square-pyramidal coordination, due to its 16 VE configuration. The square-pyramidal coordination is favored in most cases.[24]

Alkyne−CO Insertion Pathways. Instead of exchanging with a molecule of ethylene, **4** can proceed via a coupling between a CO molecule and the coordinating acetylene to yield a ruthenacyclobutenone ring. Then, the binding of a molecule of ethylene and its insertion plus a reductive elimination will lead to the cyclopentenone product. Figure 3 shows the free energy profile for this pathway. Since the coordinating acetylene and the metal center form a three-membered metallacycle, the coupling between the CO molecule and the acetylene is considered as a migratory insertion reaction of CO into the metal carbon bond. (Hereafter, we designate this pathway a CO insertion pathway.) The barrier for the insertion of an axial CO, quite unexpectedly, is as low as about 13.9 kcal/mol. It is quite unlikely for the equatorial carbonyl to insert, as reflected by the high barrier, about 39.3 kcal/mol. The intermediate **15** is only about 4.4 kcal/mol less stable than **4**, which is also very surprising since a four-membered ring suffers from a severe ring strain. The following binding of an ethylene increases the free energy by about 4.2 kcal/mol. The activation free energy for the ethylene insertion is about 16.1 kcal/mol, and about 34.7 kcal/mol overall. The resulting intermediate **18** is about 0.4 kcal/mol more stable than **3**, and the direct reductive elimination requires less than 10 kcal/mol. Thus the rate-determining step is the ethylene insertion. The overall activation free energy of the CO-insertion pathway is calculated to be 7.2 kcal/mol more favorable than that for the oxidative coupling between an ethylene and an acetylene. This significant difference strongly indicates the possibility of an alternative pathway to the traditional coupling pathway. Conceivably, **18** can bind another incoming CO to form **18-a**, which stabilizes the system by about 5.4 kcal/mol only due to the deterioration of the η^3-binding mode in **18**. The following reductive elimination requires about 21.9 kcal/mol, rendering this pathway unfavorable.

Ru−C═C Insertion versus Ru−C(O) Insertion. Clearly, there are two bonds into which the ethylene can insert. Instead of inserting into the Ru−C═C bond, the ethylene can also insert into the Ru−C(O) bond. Interestingly, this latter insertion has an even lower barrier. The overall activation free energy of this insertion is only about 29.3 kcal/mol (Figure 3b), which is 12.6 kcal/mol lower than that of the coupling between the acetylene

(21) Theoretical calculations: (a) Yamanaka, M.; Nakamura, E. *J. Am. Chem. Soc.* **2001**, *123*, 1703. (b) Milet, A.; Gimbert, Y.; Konya, D.; Greene, A. E. *J. Am. Chem. Soc.* **2001**, *123*, 5396. (c) De Bruin, T. J. M.; Milet, A.; Robert, F.; Gimbert, Y.; Greene, A. E. *J. Am. Chem. Soc.* **2001**, *123*, 7184. (d) De Bruin, T. J. M.; Milet, A.; Greene, A. E.; Gimbert, Y. *J. Org. Chem.* **2004**, *69*, 1075. (e) Lagunas, A.; Payeras, A. M.; Jimeno, C.; Pericas, M. A. *Org. Lett.* **2005**, *7*, 2033. (f) Del Valle, C. P.; Milet, A.; Gimbert, Y.; Greene, A. E. *Angew. Chem., Int. Ed.* **2005**, *44*, 5717. (g) De Bruin, T. J. M.; Michel, C.; Vekey, K.; Greene, A. E.; Gimbert, Y.; Milet, A. *J. Organomet. Chem.* **2006**, *691*, 4281. (h) Pitcock, W. H.; Lord, R. L.; Baik, M. H. *J. Am. Chem. Soc.* **2008**, *130*, 5821.

(22) Huang, J.; Hedberg, K.; Davis, H. B.; Pomeroy, R. K. *Inorg. Chem.* **1990**, *29*, 3923.

(23) (a) Li, J.; Schreckenbach, G.; Ziegler, T. *J. Am. Chem. Soc.* **1995**, *117*, 486–494. (b) Bogdan, P.; Weitz, E. *J. Am. Chem. Soc.* **1990**, *112*, 639. (c) Bogdan, P.; Weitz, E. *J. Am. Chem. Soc.* **1989**, *111*, 3163.

(24) Albright, T. A.; Burdett, J. K.; Whangbo, M.-H. *Orbital Interactions in Chemistry*; Wiley: New York, 1985.

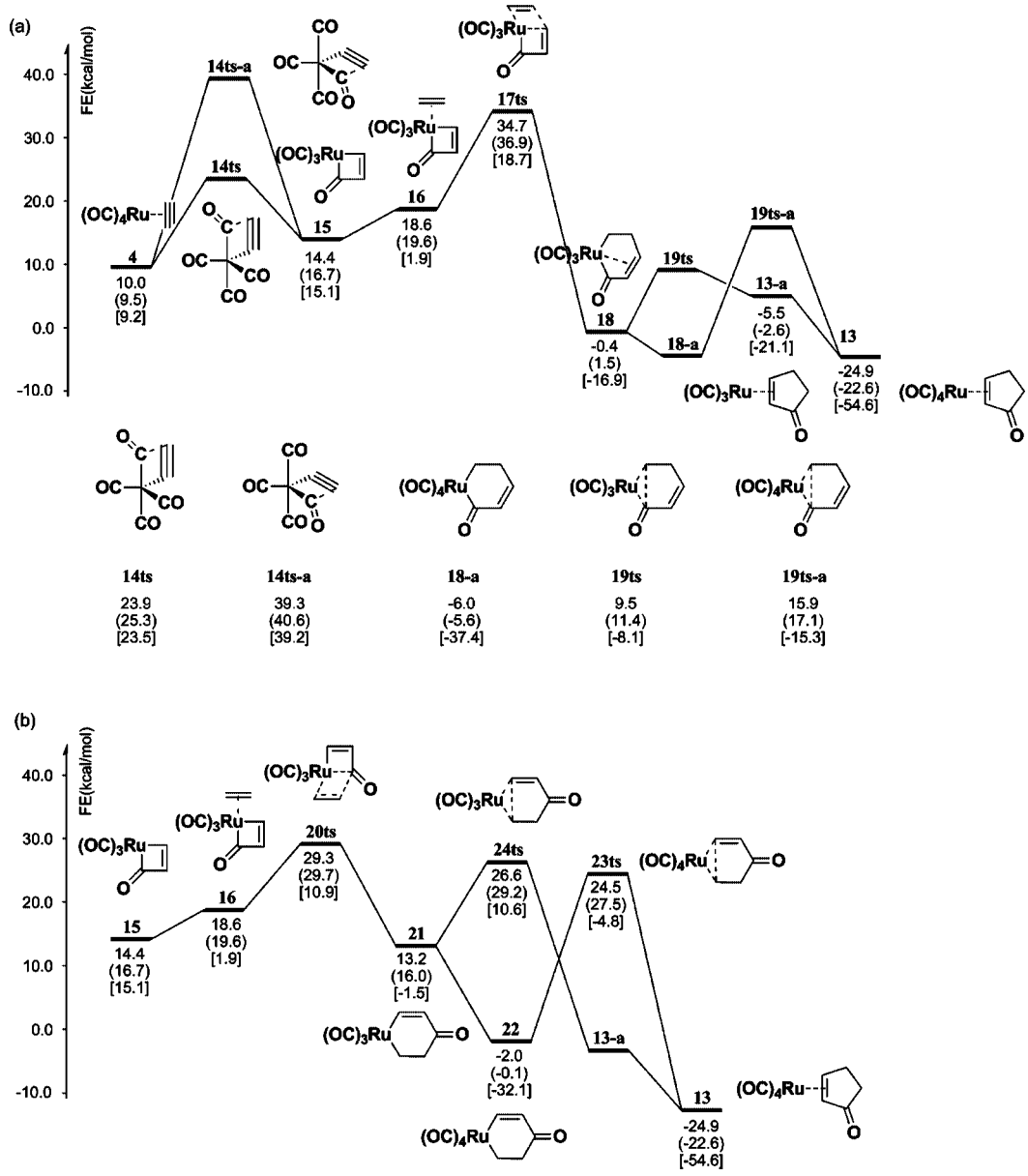

Figure 3. Free energy profile of the CO-insertion pathway.

and the ethylene. The subsequent reductive elimination might occur in two fashions, as depicted before, direct reductive elimination or reductive elimination after capturing another CO. Both pathways have similar barriers, with the latter having a barrier about 2.1 kcal/mol lower. The CO-insertion step should be the rate-determining step and the reaction should be facile. However, since the reaction was actually carried out with enynes, there should be considerable distortion for the insertion into the Ru−C(O) bond (*vide infra*). Therefore, in the real system the insertion into the Ru-C═C bond actually predominates.

Figure 4 shows the optimized structures for the CO-insertion pathway. In transition state **14ts**, the position of the acetylene only slightly changes, while one of the apical CO ligands tilts toward the carbon on the acetylene. The departing carbon of the acetylene is about 1.862 Å from the bond-forming carbon of the CO and about 2.287 Å from the metal center. The surprisingly low barrier can be understood from the frontier orbitals of reactant **4**. As shown in Figure 5, the canonical highest occupied molecular orbital (HOMO) of **4** results from the bonding interaction of the acetylene's π orbital with the metal's hybridized spd orbital, in which most electron density will localize in the C−Ru bond region. The lowest unoccupied molecular orbital (LUMO) is one set of the apical π^* orbitals of the carbonyls. Upon approaching the acetylene carbon, the electrons in the HOMO move directly to the LUMO, leading to a relatively low barrier. In addition, the HOMO−1 is an antibonding orbital comprising one metal d orbital and the vertical π orbital of the acetylene. Accordingly, there should be a bonding orbital between these two orbitals, indicating a four-electron−two-orbital interaction, which causes repulsion. When one end of the acetylene moves away, the repulsion should diminish. At the same time, the corresponding π^* orbital of the acetylene, which does not interact with the metal d orbital due to zero overlap, now mixes into the π−d bonding, stabilizing both the bonds. Thus, the transformation of **4** into **15** is not very endothermic, and there should be substantial equilibrium between the two compounds.

The incoming ethylene binds loosely with **15**, which is reflected by the low binding energy and the long bond length between the ethylene carbons with the metal as in **15**. The alkene is aligned along the Ru−C(O) bond in **15**, probably due to the smaller repulsion with the π electrons on the acyl carbon than

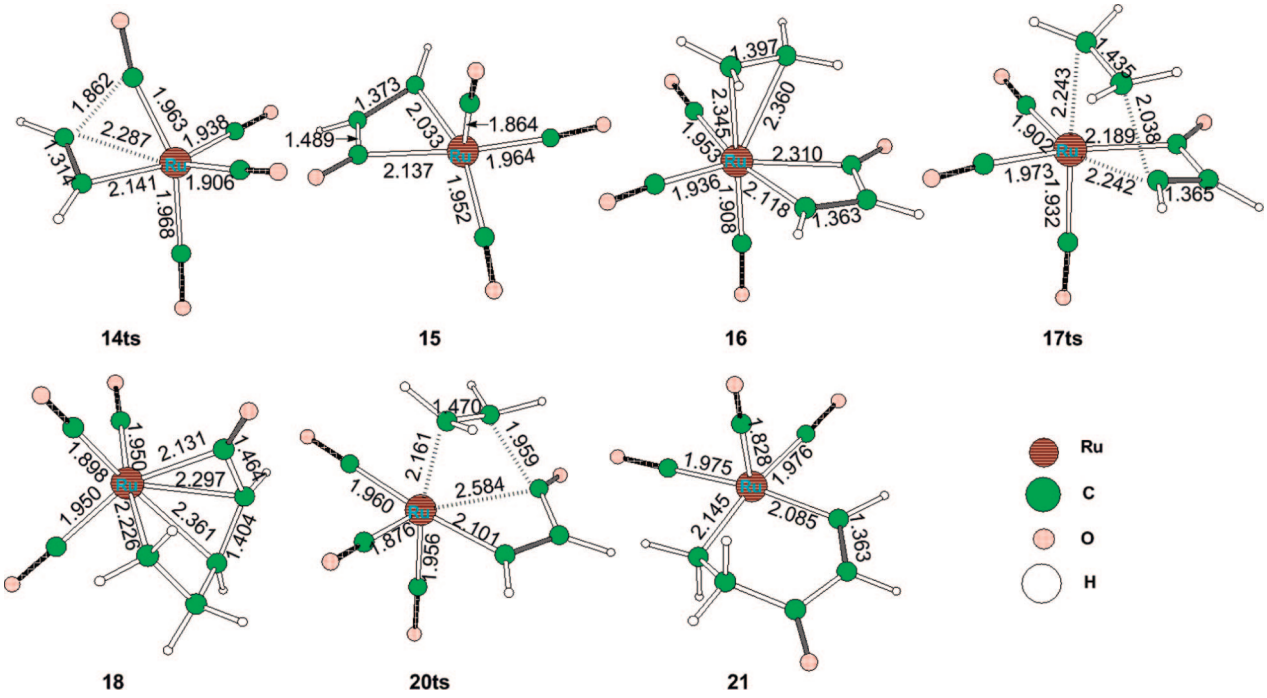

Figure 4. Structures for the CO-insertion pathway.

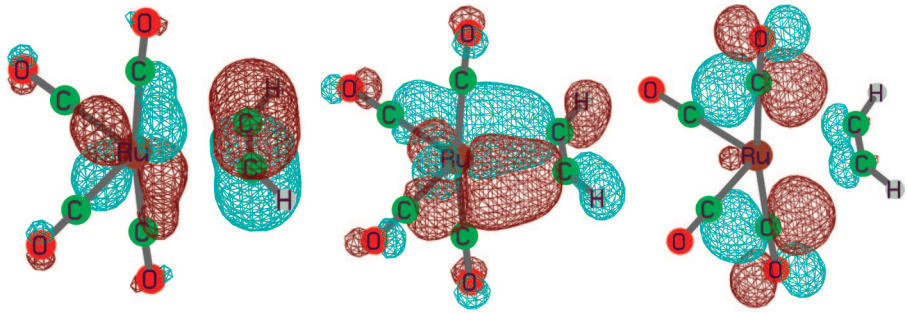

Figure 5. Frontier orbitals and the orbital energies of **4** (isovalue = 0.05).

on the alkenyl carbon. In the insertion transition state **16ts**, one of the ethylene carbons is immediately above the metal center, while the other carbon approaches the akenyl carbon. The bond length of the ethylene changes from about 1.397 Å to about 1.435 Å in the transition state. The insertion product **17** features a η^3-binding mode of the acyl carbon and the alkenyl carbons with the metal center due to the accessible π electrons and the vacant site on the metal. The η^3 binding also facilitates the reductive elimination (**18ts**) due to the coordination of the π bond. There is an agostic H bond on the saturated α position of the cyclopentenone.

Preference of Alkene Insertion into Ru−C(O). The **19ts** structure features a very long Ru−C(O) distance, as shown in Figure 4. As stated before, the insertion of ethylene into the Ru−C(O) bond is favored by about 5.4 kcal/mol over that into the Ru−C═C bond. We can understand this from the frontier orbitals of the molecule. As shown in Figure 6, the HOMO of the fragment of **15** without ethylene has a large lobe in the Ru−C(O) bond region, whereas no visible density can be seen in the Ru−C═C bond region at the isovalue of 0.05. The Ru−C═C bond actually comprises a large part of HOMO−4, which is about 2.2 eV lower in orbital energy.

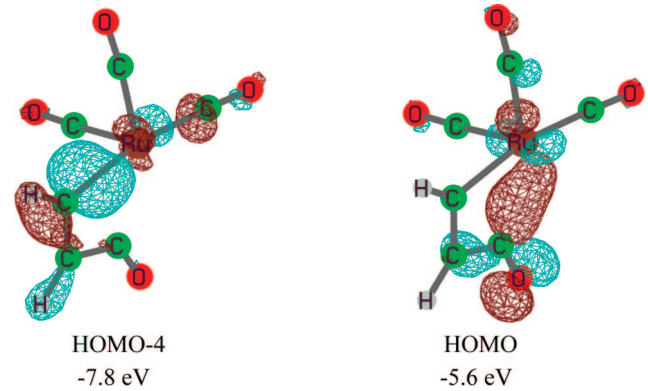

Figure 6. Frontier orbitals of the fragment that interact with ethylene in **15** (isovalue = 0.08).

1.2. [2+2+1+1] Cycloadditions. Instead of binding a molecule of ethylene, **15** can also bind another molecule of CO, yielding the 18 VE compound **25**, which is 11.5 kcal/mol more stable in terms of free energy (Figure 7a). Then, one of the carbonyls on **25** can insert into the Ru−C═C bond via **26ts** to yield **27**. The reaction barrier is calculated to be 12.6 kcal/mol, and **27** is about 1.9 kcal/mol more stable than **25**. Structure **27**

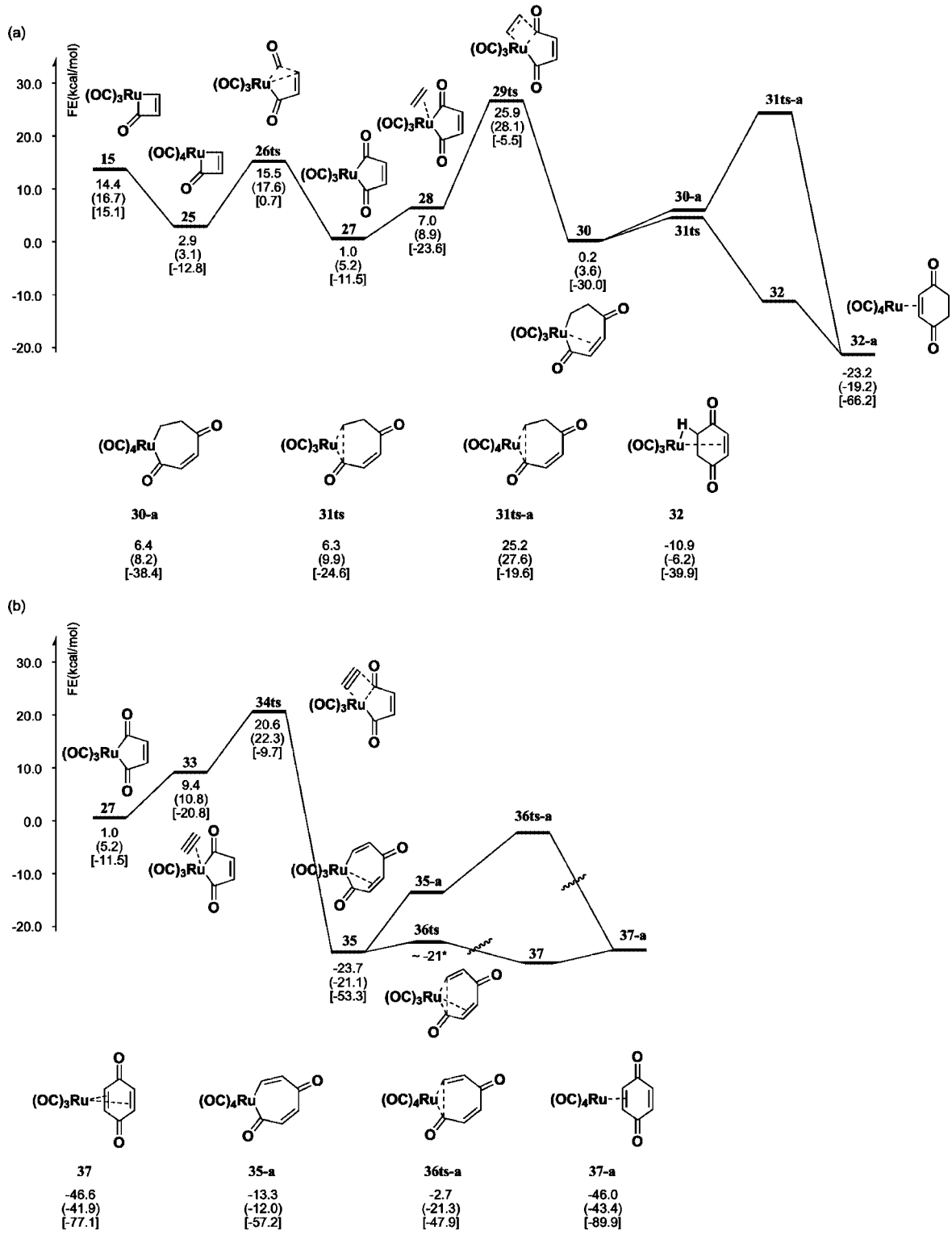

Figure 7. Free energy profiles of the [2+2+1+1] cycloadditions. *The relative free energy of **36ts** was estimated from the transition structure of the B3LYP-optimized structure, since all attempts to locate the transition structure by BP86 failed. The wave-lines suggest that the products are not in the same energy scale.

has been proposed to be an important intermediate in many reactions including the current reaction.[26] Although **27** is coordinatingly unsaturated, it lies only about 1.0 kcal/mol higher than the reactant **3** in terms of free energy. Capturing an incoming ethylene molecule does not further stabilize **27**. Instead, the coordination is endogonic by about 6.0 kcal/mol. The insertion of the ethylene has a barrier of about 18.9 kcal/mol, and the reaction is exogonic by about 6.8 kcal/mol. The following direct reductive elimination is facile, with a barrier of only about 6.1 kcal/mol. The product features an agostic H-bond of the α-H. The reaction free energy is calculated to be −10.9 kcal/mol. The η^3-binding mode of **30** again renders the reductive elimination very unfavorable after capturing another molecule of CO, as reflected by the high position of **31ts-a** in the free energy profile.

Acetylene Insertion Is More Favorable. Since there are also alkynes in the reaction conditions, **27** can also bind another molecule of acetylene. It is even more endogonic for **27** to bind

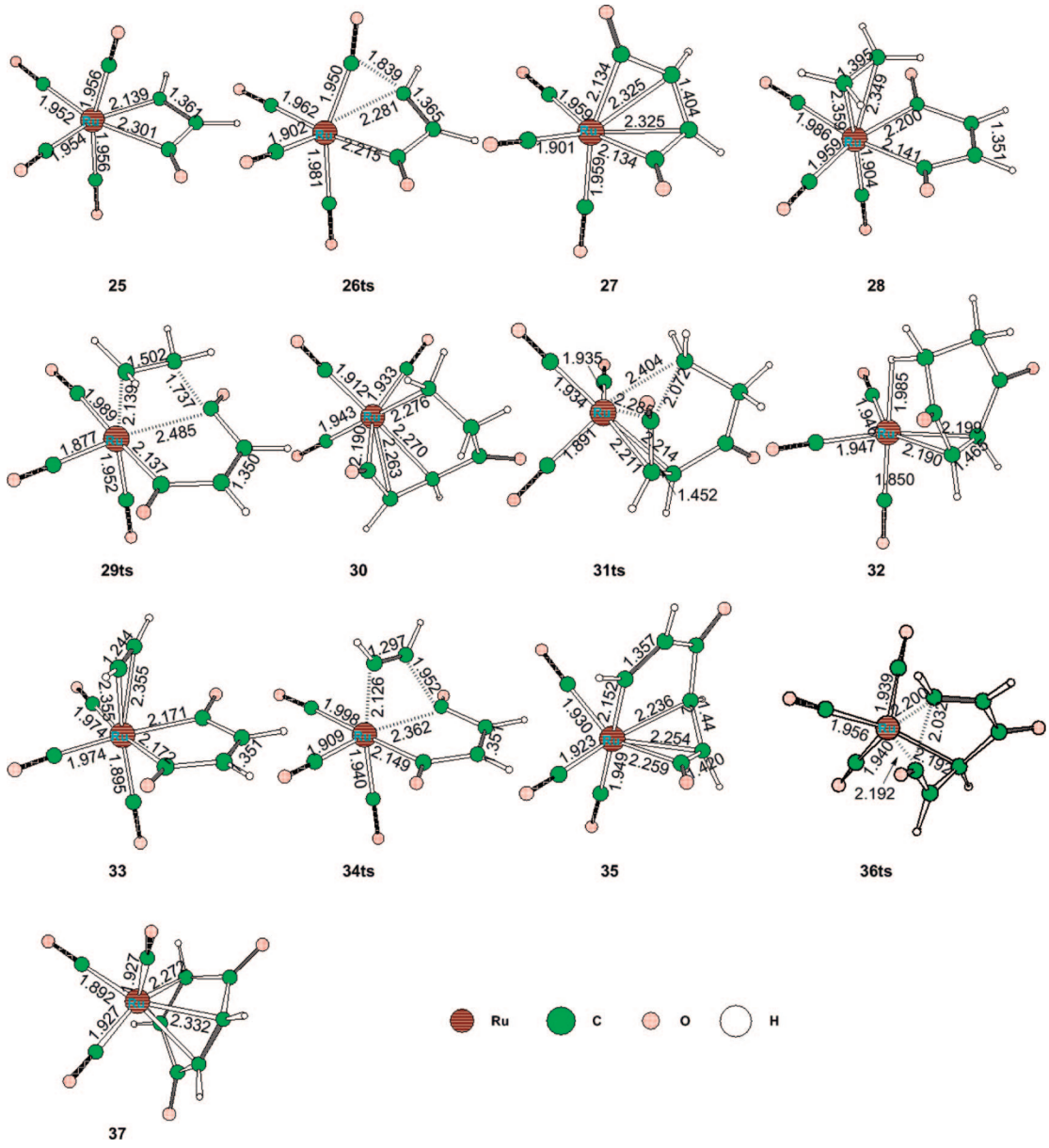

Figure 8. Key structures for the [2+2+1+1] cycloadditions.

a molecule of acetylene than to bind a molecule of ethylene. As shown in Figure 7b, **33** is about 8.4 kcal/mol less stable than **27** in terms of free energy, perhaps because ethylene has a higher HOMO. However, the insertion of acetylene into the Ru−C(O) bond is much easier than the insertion of ethylene. The insertion barrier is calculated to be as low as 11.2 kcal/mol. Moreover, the reaction is exogonic by about 33.1 kcal/mol, making this step fairly irreversible. The final reductive elimination step is even more facile, with a negligible barrier to give the final product. The overall reaction is calculated to be exogonic by 46.6 kcal/mol.

Figure 8 shows the structures in the [2+2+1+1] pathways. Structure **25** is quasi-octahedral with the apical carbonyls tilting toward the four-membered ring. The Ru−C(O) bond is lengthened upon binding of a CO molecule, and the four-membered ring becomes coplanar. Insertion of one carbonyl into the Ru−C═C bond results in the shortening of the Ru−C(O) bond as in **26ts**. Interestingly, the bond between the metal center and the carbonyl *trans* to the inserting carbonyl is elongated in the transition state. In **27**, the resulting maleoyl group coordinates to the metal center in a η^4 fashion, as indicated by the short distance between the alkene carbon and the metal center. The incoming ethylene replaces the alkene in the maleoyl group and causes the maleoyl group and the metal center to be coplanar, which might be one of the reasons why it is endogonic for **27** to bind a molecule of ethylene or acetylene. The carbonyl *trans* to the ethylene moves much closer to the metal center upon binding of the ethylene, suggesting a very loose binding of the ethylene. In transition state **29ts**, the breaking Ru−C(O) bond is elongated very much, whereas the forming C−C bond is as short as about 1.737 Å. The carbonyl *trans* to the breaking Ru−C(O) bond binds much tighter in **29ts** than in **28**, as reflected in the shortened bond length. The insertion product has a vacant coordination site. Therefore, the C═C bond coordinates to the metal center again as shown in **30**. With the advantage of the η^3-binding mode, **31ts** has a well-arranged transition state with the alkyl carbon relatively far away from the metal center (about 2.404 Å). In the product **32**, the agostic hydrogen is in the axial position, with a distance of about 1.985 Å.

Scheme 4. Orbital Interactions in the Insertion of Acetylene

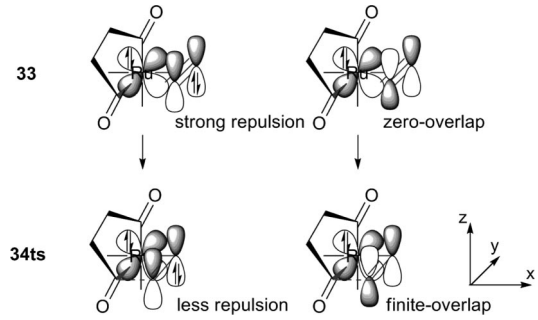

When an acetylene binds to **27**, the same thing occurs with the ethylene. The *trans* CO binds even tighter than in **33**, indicating a weaker bonding between acetylene and the metal than between the ethylene and the metal. However, in the transition state (**34ts**), the Ru−C(O) bond is not so long and the forming C−C bond is longer than that for the ethylene. The resulting intermediate also has a η^3-binding mode as in **35**. In the product **37**, the quinone binds the metal center with its two double bonds.

Favorable Acetylene Insertion. There are two reasons why acetylene inserts more easily than ethylene into the Ru−C(O) bond. On one hand, the compression of the C−C σ bond is more severe in acetylene than in ethylene, leading to a stronger driving force for the acetylene to insert.[25] On the other hand, there might be some orbital interactions involved in the acetylene insertion. The noncoordinating vertical π bond of the acetylene is repulsive toward one of the metal d orbitals. When the insertion occurs, the vertical π bond slips aside and diminishes the repulsion. Furthermore, upon moving aside, the vertical π^* bond of the acetylene begins to interact with the metal d orbitals. As shown in Scheme 4, the π bond is in-phase with the d_{xz} orbital of the metal center. However, both orbitals are occupied orbitals and there arises repulsion. In the transition state, the repulsive interaction is not so severe as that in the reactant. For the π^* orbital, there is no interaction in the complex due to cancelation of the overlap in opposite phases. In the transition state however, the d_{xz} orbital overlaps with only one lobe of the π^* orbital, so that the interaction is favorable and the system is stablized.

2. Studies of Real Systems. Real System for Pauson−Khand-Type Reaction. To ensure that our study of model reactions faithfully reflects the situation of the real system, we also calculated the key structures of the intramolecular reactions. Figure 9 shows the free energies of the structures that will determine the reaction pathway. Since all the energies are relative to the same reference compound, we can directly compare the energy difference between the intermolecular reactions and the model intramolecular reactions.

In the coupling pathway, the gain of translational entropy of **39** makes it about 4.8 kcal/mol more stable than **5** in terms of free energy. However, the coupling step has a larger barrier in the intramolecular reaction than in the intermolecular reaction, probably due to the unfavorable conformation for the fused five-membered ring in the transition structure (Figure 10). The overall activation free energy still amounts to about 39.2 kcal/mol. The dihedral angle of $C_a-C_b-C_c-C_d$ is about −5.6° in **40**, while there is no such near-eclipse conformation in **43ts**, which explains the larger difference in the overall activation free energy of the alkene−alkyne coupling pathway and the CO-insertion pathway.

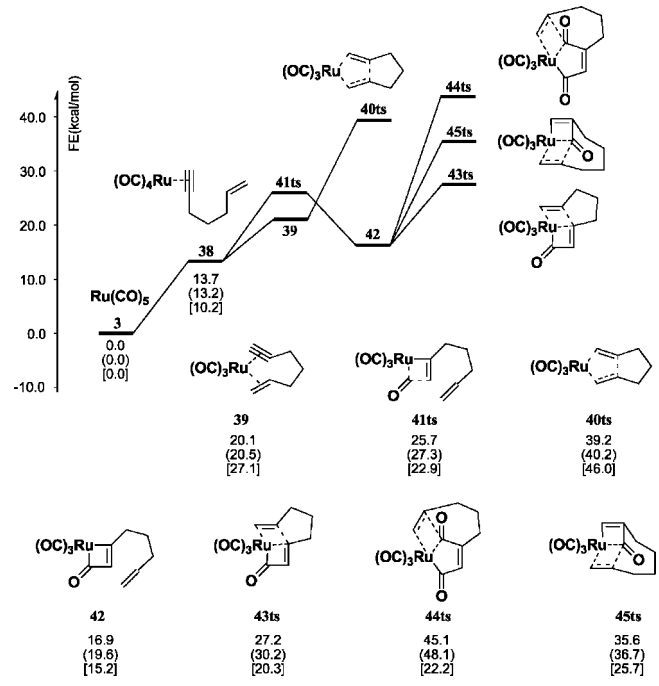

Figure 9. Free energy profile of the intramolecular situation.

For the CO-insertion pathway, the insertion of CO (**41ts** to **38**) has a smaller barrier compared with that in the intermolecular reaction, which counteracts the unfavorable coordination of the acetylene and leads to a similar activation free energy for the formation of the metalla-, four-membered ring.

The subsequent insertion of alkene is very different due to the geometrical constraints. The transition state of the alkene insertion into the Ru−C(CO) bond is severely distorted, as shown in Figure 10. The forming C−C bond is now much shorter in the intramolecular transition state than in the intermolecular one, which reflects the late-transition character of the reaction and therefore shows a large barrier. The insertion into the Ru−C═C bond does not suffer from such distortion. In contrast, the conformation for the fused five-membered ring is actually very similar to that for the free five-membered ring. Thus, in the intramolecular version, the barrier for the insertion of the double bond into the Ru−C═C bond is much lower than that into the Ru−C(O) bond.

When another CO inserts into the Ru−C═C bond to form the maleoyl five-membered ring, the enyne has to distort to an even more unfavorable position to insert into the Ru−C(O) bond. The activation free energy for **44ts** is calculated to be 45.1 kcal/mol, which forbids the formation of quinones or hydroquinones. Also, we should note that the product would be extremely unstable due to the unfavorable conformation if quinones and hydroquinones were to form. To summarize, for the intramolecular reaction, the Pauson−Khand-type reaction should proceed through the CO-insertion pathway in a way that

(25) (a) Cheng, M.-H.; Lee, G.-H.; Peng, S.-M.; Liu, R.-S. *Organometallics* **1991**, *10*, 3600. (b) Cheng, M.-H.; Syu, H.-G.; Lee, G.-H.; Peng, S.-M.; Liu, R.-S. *Organometallics* **1993**, *12*, 108. (c) Mao, T.; Zhang, Z.; Washington, J.; Takats, J.; Jordan, R. B. *Organometallics* **1999**, *18*, 2331. (d) Barrow, M.; Cromhout, N. L.; Cunningham, D.; Manning, A. R.; McArdle, P. *J. Organomet. Chem.* **2000**, *612*, 61. (e) Barrow, M.; Cromhout, N. L.; Manning, A. R.; Gallagher, J. F. *J. Chem. Soc., Dalton Trans.* **2001**, 1352. (f) Elarraoui, A.; Ros., J.; Yáñez, R.; Solans, X.; Font-Bardia, M. *J. Organomet. Chem.* **2002**, *642*, 107.

(26) Dewar, M. J. S. *The Molecular Orbital Theory of Organic Chemistry*; McGraw-Hill: New York, 1969.

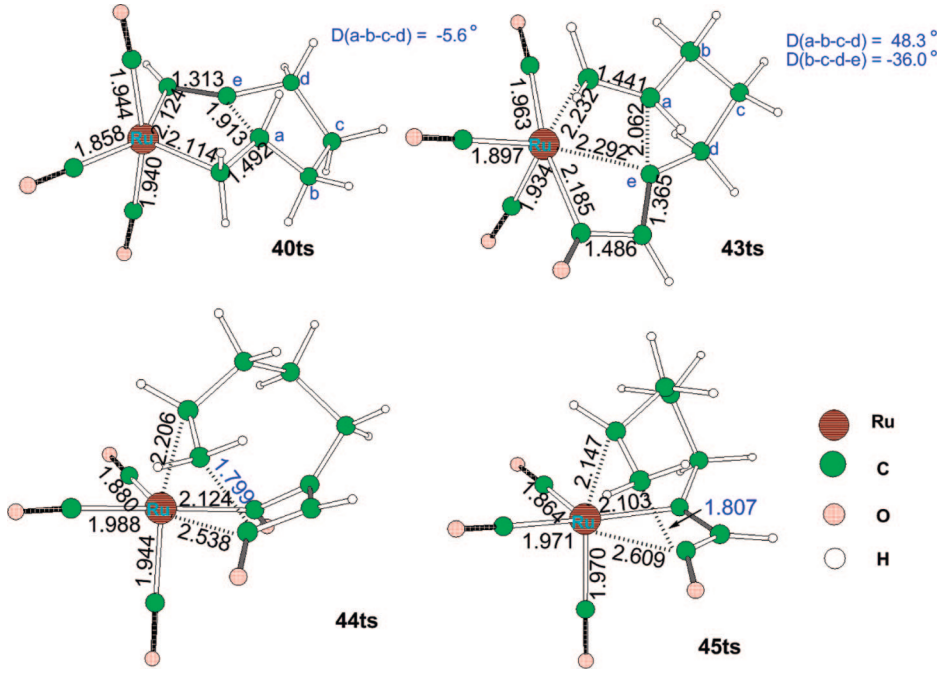

Figure 10. Key structures of the intramolecular situation.

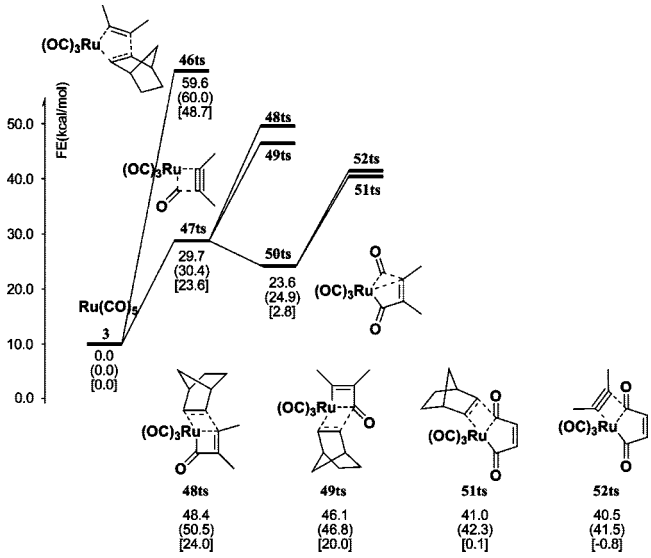

Figure 11. Energetics of the real [2+2+1+1] system.

features the insertion into the Ru−C═C bond. The quinone and hydroquinone formation is not possible due to the high reaction barrier.

Real System for [2+2+1+1] Cycloadditions. The model calculations favored the quinone formation. However, a significant amount of hydroquinone was formed in the reaction. We believe that this occurs because of the strained alkenes and substituted alkynes used as reactants. Figure 11 shows the energetics of key transition structures of the considered pathways. Though the calculated activation free energies are much higher than those of our model calculations, the trends are very similar. The oxidative coupling pathway still presents the highest barriers, whereas the [2+2+1+1] cycloadditions have the lowest activation free energies. The increased barriers are believed to partly arise from the steric repulsion of the methyl group on alkyne and the larger size of norbornene compared with ethylene. The final insertion of the [2+2+1+1] pathways is not in favor of the alkyne insertion any more, as **53ts** now has almost the same overall activation free energy with **52ts**, about 40.5 and 41.0 kcal/mol, respectively. Besides, the high activation free energies are also believed to originate from overestimation of the entropy loss, as the reactants are all in liquid phase.

Polarization of the Methyl Group on the Alkyne. It has been pointed out that polarization of alkynes can substantially influence the selectivity of the Pauson−Khand reaction;[21c,g] we therefore investigated the possible effects of substitution on the alkyne in the Ru-catalyzed Pauson−Khand-type reaction. Figure 12 shows the relative energies and free energies of the key structures in the reaction pathway. We found that the methyl substituent contributes little to the selectivity of the alkyne−alkene coupling pathway. The **53ts** has a free energy almost the same as that of **54ts**. The equatorial coupling transition structures **53ts-a** and **54ts-a** still have activation free energies higher than those of **53ts** and **54ts**. In the CO-insertion pathway, it was found that a regioselectivity contrary to that of the original Pauson−Khand reaction might be obtained, though the selectivity might be small. In other words, the methyl substituent will be found at the β position in the cyclopentenone product, since **57ts** lies slightly lower than **58ts** in terms of free energy. Moreover, the CO-insertion pathway still has a significantly lower barrier than the alkyne−alkene coupling pathway.

Conclusion

We have studied the mechanism of a series of cycloaddition reactions between alkenes, alkynes, and CO catalyzed by a Ru complex by DFT calculations. The results show that the mechanisms are significantly different for inter- and intramolecular cycloadditions under similar conditions. For the intramolecular reactions, the Pauson−Khand-type [2+2+1] reaction will occur, while for the intermolecular reactions, two competitive [2+2+1+1] cycloadditions will proceed.

An alternative mechanism has been proposed for the Pauson−Khand-type reaction to the traditional oxidative cou-

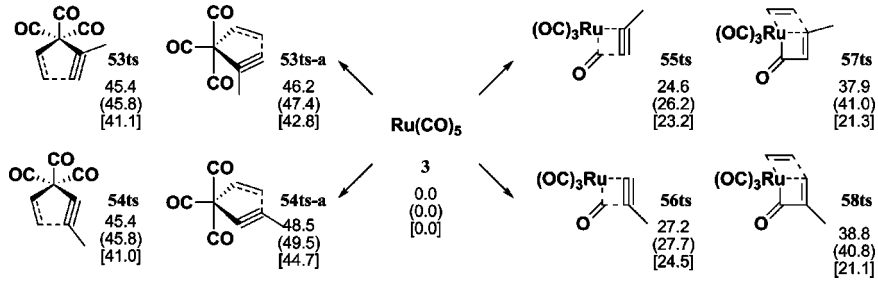

Figure 12. Effects of methyl substituent in the alkyne on the selectivity and reaction.

pling pathway. We found that the newly proposed CO-insertion pathway has a significantly lower activation free energy and also shares a few intermediates with the [2+2+1+1] cycloaddition pathways.

We compared all these mechanisms and found that insertion into the Ru−C(O) bond is easier than into the Ru−C═C bond, due to the flexible nature of Ru−C(O) bond. We also found that the insertion of acetylene into the Ru−C(O) bond is easier than that of ethylene because acetylene binds the metal looser and its π electrons have strong repulsion with the metal center.

We hope our study will shed some light on the chemistry of similar cycloaddition reactions[27] and will facilitate future exploration of the catalyst.

Acknowledgment. We are grateful to the National Natural Science Foundation of China (20225312) and the Research Grants Council of Hong Kong (N_HKUST 623/04) for financial support of the research.

Supporting Information Available: A PDF file containing calculated energetics and Cartesian coordinates of all computed structures is available free of charge via the Internet at http://pubs.acs.org.

OM8004178

(27) (a) Kondo, T. *Synlett.* **2008**, *5*, 629. (b) Kondo, T.; Nomura, M.; Ura, Y.; Wada, K.; Mitsudo, T. *J. Am. Chem. Soc.* **2006**, *128*, 14816. (c) Kondo, T.; Nakamura, A.; Okada, T.; Suzuki, N.; Wada, K.; Mitsudo, T. *J. Am. Chem. Soc.* **2000**, *122*, 6319. (d) Kondo, T.; Kaneko, Y.; Taguchi, Y.; Nakamura, A.; Okada, T.; Shiotsuki, M.; Ura, Y.; Wada, K.; Mitsudo, T. *J. Am. Chem. Soc.* **2002**, *124*, 6824. (e) Morisaki, Y.; Kondo, T.; Mitsudo, T. *Org. Lett.* **2000**, *2*, 949.